Tubular alumina formed by anodization in the meniscal region

S. K. Lazarouk,[1,a)] D. A. Sasinovich,[1] V. E. Borisenko,[1] A. Muravski,[2] V. Chigrinov,[2] and H. S. Kwok[2]

[1]*Belarusian State University of Informatics and Radioelectronics, P. Browka 6, 220013 Minsk, Belarus*
[2]*Center for Display Research, Hong Kong University of Science and Technology, Clear Water Bay 190, Hong Kong*

(Received 31 August 2009; accepted 5 January 2010; published online 12 February 2010)

A method to fabricate tubular nanoporous alumina layers by anodization of aluminum at current densities up to 1400 mA/cm^2 and anodization rates up to 70 μm/min has been developed. It implies anodization in the meniscal region of the sample dipping into an electrolyte. The formed porous alumina has been found to be selforganized nanotube cells when the anodization current excides 100 mA/cm^2. The formation of nanotubes is supposed to be controlled by the increased volume expansion factor (more than 2) at high forming current densities. The meniscal anodization allows fabrication of porous alumina nanotubes with desired tilt angles in the range of 0°–16°.
© *2010 American Institute of Physics*. [doi:10.1063/1.3305672]

I. INTRODUCTION

Self-organization during electrochemical anodization of metals and semiconductors is a promising way to fabricate ordered nanoporous structures. Anodic porous alumina is a well-known self-ordered nanoporous material formed by anodization of aluminum in an appropriate acidic solution.[1–3] Recently, Chu *et al.*[4] showed an appearance of ordered tubular nanoporous alumina films by high current (~200 mA/cm2) anodization in the sulfuric acid electrolyte in the temperature range of 0.1–10 °C with vigorous magnetic stirring. The anodization below room temperature is unavoidably accompanied by obvious technological restrictions related to processing of large area samples.

In this paper we present a simple approach to fabricate large area ordered nanoporous tubular alumina films at room temperature but at high current densities reaching 1400 mA/cm^2. The main idea of our approach is to perform anodization in a meniscal region of the sample dipping into an electrolyte. Such an approach provides an effective heat sink from the anodization zone thus preventing overheating effects. Moreover, porous alumina with tilt pores can be formed by anodization in the meniscal region. The nanoporous layers with controllable tilt angles of pores are important for fast and stable liquid crystal (LC) displays.[5,6] So far, we have also focused on the regimes of the anodic technique to fabricate nanoporous structures with tilted pores.

II. EXPERIMENTAL

Aluminum films were deposited by magnetron sputtering onto oxidized silicon wafers. The thickness of the films was ranged from 100 to 1000 nm. The anodization was performed in the 2% aqueous solution of sulphuric acid. A potentiostatic regime with forming voltages ranging from 10 to 140 V was realized providing maximum current densities of 10–1400 mA/cm^2. The main peculiarity of the anodization process consists in the electrochemical oxidation of the aluminum film in the narrow meniscal region moving over the aluminum covered sample surface during its dipping into the electrolyte at the velocity ranged from 0.1 to 1.0 mm/min, as schematically shown in Fig. 1(a). The anodization front was monitored *in situ* by optical control as illustrated in Fig. 1(b). The anodization current density was calculated by taking into account the measured anodization front width. Temperature of the meniscal region was monitored with the infrared detector "Thermovision-880" having the sensibility of 1 °C. For comparison we also measured the temperature of the anodic film during conventional full area anodization of the sample of 10 mm in diameter by using thin film resistor sensors placed between the aluminum film and the silicon substrate.

Structure of the fabricated porous alumina films were analyzed with a scanning electron microscopy (SEM). Elemental composition of the films was defined by Auger spectroscopy using the PHI-660 Perkin Elmer spectrometer after 5 min surface cleaning by 3.5 keV Ar^+ ions.

III. RESULTS AND DISCUSSION

The width of the meniscal region was observed to be of a few microns. Figure 2 shows the anodization front in the meniscal region at different forming voltages. It was found

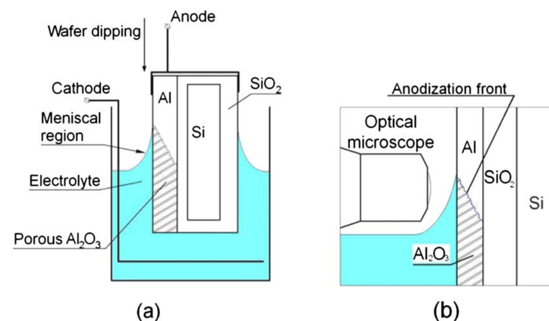

FIG. 1. (Color online) Schematic view of the anodization process in the meniscal region: (a) electrochemical cell and (b) optical control of the anodization process.

a)Electronic mail: serg@nano.bsuir.edu.by.

 © 2010 American Institute of Physics

Downloaded 23 Apr 2010 to 143.89.47.22. Redistribution subject to AIP license or copyright; see http://jap.aip.org/jap/copyright.jsp

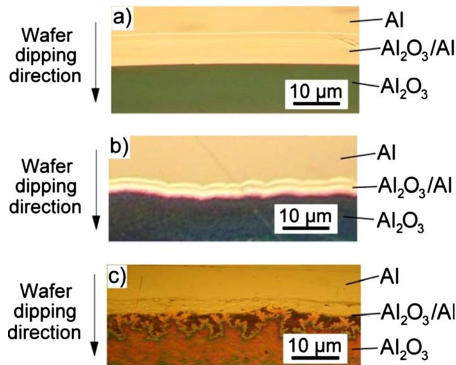

FIG. 2. (Color online) Optical microscope photographs of the aluminum anodization front in the meniscal region for different forming voltages: (a) $U_f = 100$ V, (b) $U_f = 120$ V, and (c) $U_f = 130$ V. Aluminum film thikness is 0.2 μm.

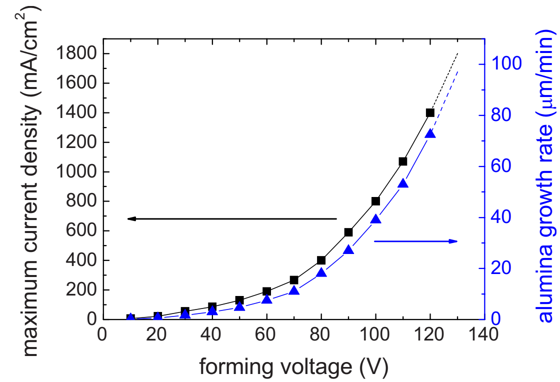

FIG. 4. (Color online) Maximum current density and alumina growth rate during meniscal anodization of aluminum films as a function of the forming voltage.

that the anodization front is homogenous at forming voltage up 100 V [Fig. 2(a)]. Some heterogeneity in the anodization front appears at 120 V [Fig. 2(b)], while anodization at 130 V results in the local breakdown in the anodization area which makes it difficult to estimate precisely the anodization area [Fig. 2(c)].

Figure 3 presents images of the samples after meniscal anodization at various forming voltages. The meniscal anodization at 100 V provides fabrication of rather uniform porous alumina films. Meantime, the meniscal anodization at 120 V results in porous oxide films with linear fringes originated from local breakdowns during the anodization process.

Figure 4 presents the current density dependence on the forming voltage for the porous anodization process. The dashed lines correspond to the regimes accompanied with local thermal breakdowns in the growing porous alumina. Note that in the case of conventional full area anodization local breakdowns occur at forming voltages more than 35 V, while local breakdowns during meniscal anodization are observed at 120 V and higher.

We have experimentally noticed that meniscal anodization at high current densities does not heat up the samples significantly. Figure 5 displays the measured temperature of the films being anodized during the conventional full area and meniscal anodization processes. Heating of the anodization zone in the meniscal region is evident to be considerably decreased. It should be noted that these data were obtained without electrolyte stirring. When intense electrolyte stirring was used, the heating effect was reduced only for conventional full area anodization while for meniscal anodization we could not observed any decrease in the temperature. It means that the heat sink in the case of meniscal anodization is more effective.

Anodization in the meniscal region along with the record values of the forming voltages and current densities demonstrates extremely high growth rates of porous alumina. In particular, according to[4,7] the highest parameters achieved for sulphuric electrolytes were 70 V, 500 mA/cm^2, and 3 μm/min, respectively. We have reached 120 V, 1400 mA/cm^2, and 70 μm/min (Fig. 4).

Porous anodization at high forming voltages and current densities has been found to be accompanied with unusually high volume expansion factor (Fig. 6). It was found to reach 3.1 that is almost twice larger than previously reported maximum values [(1.6–1.7) (Ref. 8)]. Such high volume expansion factor is supposed to be caused by an enlarged sulfur content inside the porous alumina formed at high electric fields. The sulfur concentration in the porous alumina formed at 80 V was measured to be about 10%, meantime in the porous alumina formed at 20 V it was less than 3%. The difference can be explained by an enhanced electrolyte anion incorporation into porous alumina during the much faster meniscal anodization process. The high forming voltage pro-

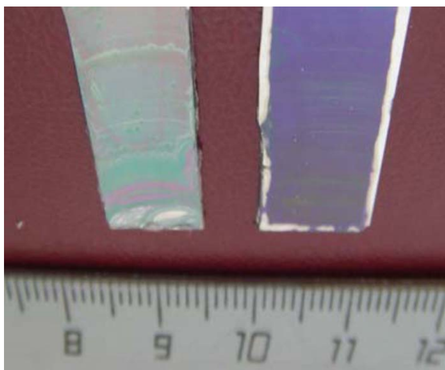

FIG. 3. (Color online) The alumina films fabricated by meniscal anodization at forming voltages 100 V (right) and 120 V (left).

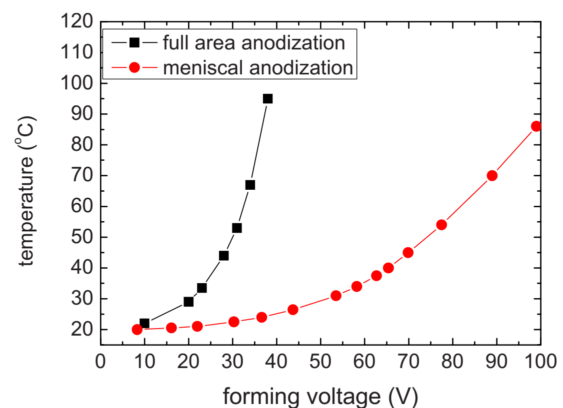

FIG. 5. (Color online) The temperatures measured in the anodic zone during anodization of aluminum films at different forming voltages.

Downloaded 23 Apr 2010 to 143.89.47.22. Redistribution subject to AIP license or copyright; see http://jap.aip.org/jap/copyright.jsp

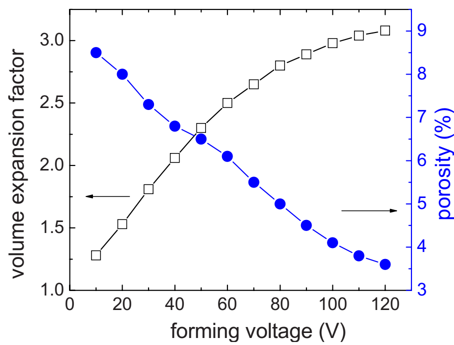

FIG. 6. (Color online) Volume expansion factor and porosity of alumina fabricated by meniscal anodization of aluminum films as a function of the forming voltage.

motes this effect. The high volume expansion also results in low porosity of alumina, which is about 3%. This is smaller than known minimal porosity of 5% for a sulphuric electrolyte.[4] In addition, porous anodization at high current densities provides formation of self-ordering structures without pretexturing treatment.[4] Figure 7 shows SEM images of porous alumina formed at 70 V where self-ordering within the porous layer thickness is evident [Fig. 7(a)]. The arrangement of pores at the alumina surface has turned out to be random [Fig. 7(b)]. Self-ordering of porous alumina has started in the bottom parts [Figs. 7(c) and 7(d)] and ordering is enhanced with an increase in the thickness of the porous alumina. The important feature during porous alumina formation at high current densities is an appearance of a nanotubular alumina structure. We have found that nanotubes are formed at current densities higher than 100 mA/cm^2. Such forming conditions also led to the volume expansion factor of 2 and higher. The enlarged volume expansion provides an enhanced mechanical tension between alumina hexagonal cells. It results in the shift in neighbor cells and divides alumina films into separated tubular cells as it can be seen in the cross section of the porous alumina films [Fig. 7(a)]. We believe that this is the main driving force for the formation of alumina nanotubes. The similar nanotubular structures were observed during porous anodization of titanium with the volume expansion factor more than 2.[9]

SEM image of the porous alumina formed at 120 V is presented in Fig. 8. The thickness of the as deposited aluminum film was 200 nm resulting in the porous alumina as thick as 630 nm. Thus, accounting for the relatively small

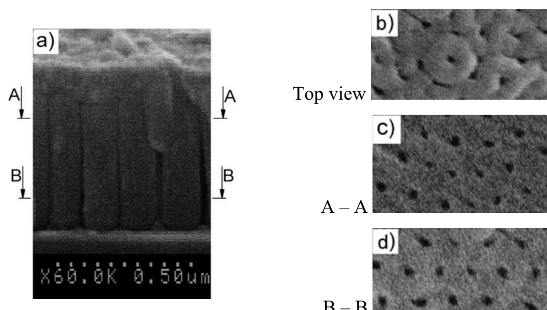

FIG. 7. SEM images of porous anodic alumina films formed by anodization of aluminum in the meniscal region at 70 V: (a) cross section, (b) top view, (c) A–A planar section, and (d) B–B planar section.

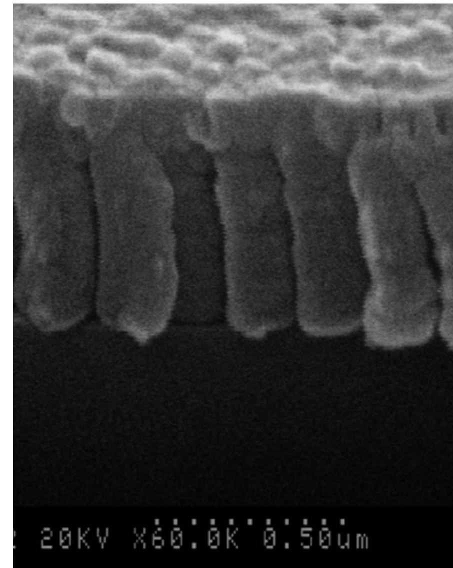

FIG. 8. SEM image of porous alumina film formed by the meniscal anodization at 120 V.

contribution of the pore volume, the volume expansion factor is estimated to be about 3.1. The interpore distance is found to be around 200 nm. To our knowledge this is the record for porous alumina formed in electrolytes based on the sulfuric acid. However, the tubular structure formed at 120 V and shown in Fig. 8 is not so regular as those formed at 70 V (Fig. 7).

The SEM investigation of the porous alumina formed at high current densities shows that the top layer has the typical porous structure while the middle and bottom layers have the tubular structure. The top layer thickness is estimated to be of about 100 nm, and it corresponds to the barrier oxide layer thickness. It means that the barrier oxide was formed first then the pores appeared inside the barrier layer and eventually the formation of the tubular structure occurred.

Thus, we have found new peculiarities of porous alumina formation with tubular structure. It allows us to propose the formation mechanism for tubular cells. The mechanism based on volume expansion of anodic alumina (the volume expansion factor should be lager than 2) which results in the shift in neighbor porous alumina cells at the border between them. Meantime, Mei *et al.*[10] consider the alumina tubular structure to be caused by the presence of voids between porous alumina cells. The reason of void appearance is a vacancy accommodation on aluminum apexes between the alumina cells. The tubular structure has been demonstrated only after chemical etching of anodic films.[10] We have observed the tubular alumina structure just after the anodization process without chemical etching (Figs. 7 and 8).

It is known that porous anodic alumina can be used as an alignment layer for vertical orientation of LC materials.[5] The alignment layer with the controlled tilt angle should be used to improve the stability of LC devices and their frequency response.[6] Previously,[11] we demonstrated that alumina films with a tilt porous structure can be formed by anodization in a meniscal region. In the current study we found high current

Downloaded 23 Apr 2010 to 143.89.47.22. Redistribution subject to AIP license or copyright; see http://jap.aip.org/jap/copyright.jsp

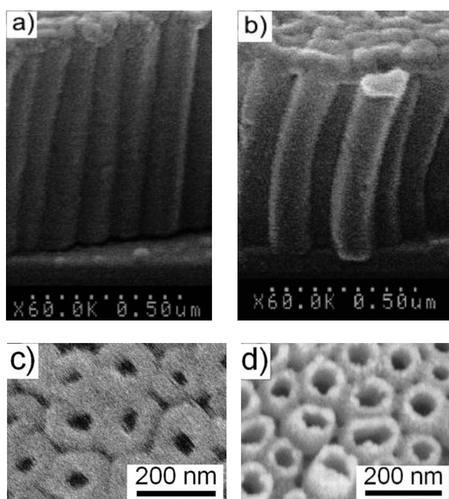

FIG. 9. Porous alumina with tilt cells formed by anodization in the meniscal region: (a) tilted cells at the angle of 7° (V_a/V_d=0.12), (b) a changing inclination of pores (the upper layer V_a/V_d=0.3, the bottom layer V_a/V_d=0.01), (c) top view after pore etching for 10 min, and (d) alumina nanotubes obtained after pore etching for 20 min.

densities providing high anodization rate (V_a). In our experiments the anodization rate was comparable with the wafer dipping velocity (V_d).

Figure 9 shows SEM images of porous alumina with tilt cells. The developed technique allows formation of the cells with linear pores tilted by a constant angle to the substrate [Fig. 9(a)] as well as with arc-type pores with the tilt angle changing from 16° at the surface up to 0° at the film/substrate interface [Fig. 9(b)]. The latter geometry can be easily realized by changing the V_a/V_d relationship during the anodization process. If necessary, the top porous layer can be removed from the porous alumina film with the tubular structure by chemical etching in 1M H_3PO_4 at 30 °C. Figure 9(c) shows the surface of the porous alumina film after 10 min of etching. The etching process occurs both inside the pores and at the film surface. The cells in the porous alumina preserve a hexagonal form. After 20 min etching closely packed alumina nanotubular structure develops as shown in Fig. 9(d). Thus, the alumina tubular structure can be fabricated by chemical etching of porous alumina samples. The tubulars in porous alumina without chemical etching have deformated external walls. The external wall form is close to the hexagonal prism structure [Fig. 9(c)]. The nanotubular alumina structures have advantages over porous and pillar structures. The inner surface of a nanotubular structure is considerably larger in comparison with porous and pillar structures providing the stable LC alignment.

Figure 10 shows the average tilt angle of the pores in the porous alumina as a function of the sample dipping velocity at different forming voltages of the meniscal anodization process. Analyzing the growth of pores at a tilt angle to the substrate surface one can estimate this angle to be $\alpha = \arcsin(V_a/V_d)$.

Comparison of the experimental data with the calculations is presented in Fig. 10. The discrepancy is less than 10%. Thus, the tilt angle can be tuned by an appropriate choice of the dipping velocity and anodization regimes. We have found experimentally that it can be varied in the range from 0° to 16° with high accuracy.

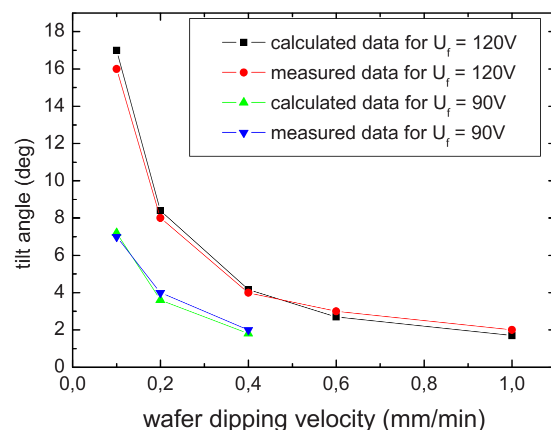

FIG. 10. (Color online) The tilt angle of alumina nanotubes vs the wafer dipping velocity.

IV. CONCLUSION

Anodization of aluminum films in the meniscal region provides unique conditions for the electrochemical processes resulting in formation of self-ordering nanoporous alumina with a tubular structure and in the controllable formation of tilted pore channels. Narrow anodization zone and effective heat sink ensure reaching of record parameters of the anodization process, which are maximum forming voltage 120 V, current density 1400 mA/cm^2, and oxide growth rate 70 μm/min. As a result, nanoporous anodic films characterizing by an enlarged volume expansion factor and reduced porosity can be fabricated. The tilt angles of the pores ranged from 0° up to 16° have been obtained by tuning the anodization regimes.

Besides already mentioned prospects of porous alumina fabricated at high forming voltages as an aligning substrate for LCs it could be also used for multilevel aluminum interconnects in very large scale integrated circuits.[12] In this case the aluminum undercutting effect is minimized by an enhanced anisotropy at high electric field anodization.[13] This approach provides planarization and high reliability of the aluminum interconnects.[14,15] Porous anodic alumina with a low porosity could be also employed as a waveguide material in interchip optical interconnects,[16] in which optical losses are reduced to an appropriate level.[17] Moreover, the anodic alumina with low porosity is an effective surface passivating material for semiconductor diodes fabricated in silicon.[18,19]

ACKNOWLEDGMENTS

This work partially has been supported by the Belarus National Fund of Fundamental Researches (Research Project No. 09–7016). The authors thank Dr. Migas D. for his help.

[1]H. Masuda, H. Yamada, M. Satoh, H. Asoh, M. Nakao, and T. Tamamura, Appl. Phys. Lett. **71**, 2770 (1997).
[2]G. E. Thompson, Thin Solid Films **297**, 192 (1997).
[3]F. Zacharatos, V. Gianneta, and A. G. Nassiopoulou, Nanotechnology **19**,

Downloaded 23 Apr 2010 to 143.89.47.22. Redistribution subject to AIP license or copyright; see http://jap.aip.org/jap/copyright.jsp

495306 (2008).
[4]S. Chu, K. Wada, S. Inoue, M. Isogai, and A. Yasumori, Adv. Mater. **17**, 2115 (2005).
[5]T. Maeda and K. Hiroshima, Jpn. J. Appl. Phys., Part 2 **43**, L1004 (2004).
[6]S. Lazarouk, A. Muravski, D. Sasinovich, V. Chigrinov, and H. S. Kwok, Jpn. J. Appl. Phys., Part 1 **46**, 6889 (2007).
[7]P. Y. Deng, X. D. Bai, X. W. Chen, and Q. L. Feng, J. Electrochem. Soc. **151**, B284 (2004).
[8]I. Vrublevsky, V. Parkoun, V. Sokol, J. Schreckendach, and G. Marx, Appl. Surf. Sci. **222**, 215 (2004).
[9]D. Gong, C. Grimes, O. Varghese, W. Hu, R. Singh, Z. Chen, and E. Dickey, J. Mater. Res. **16**, 3331 (2001).
[10]Y. F. Mei, X. L. Wu, X. F. Shao, G. S. Huang, and G. G. Siu, Phys. Lett. A **309**, 109 (2003).
[11]D. Sasinovich, P. Katsuba, and S. Lazarouk, Injenernyi Vestnik **1(21)/1**, 172 (2006).
[12]S. Lazarouk, I. Baranov, G. Maello, E. Proverbio, G. De Cesare, and A. Ferrari, J. Electrochem. Soc. **141**, 2556 (1994).
[13]D. A. Brevnov, R. L. Womack, P. Atanassov, G. P. López, T. M. Bauer, Z. A. Chaudhury, C. D. Schwappach, and L. E. Mosley, J. Electrochem. Soc. **153**, B108 (2006).
[14]S. Lazarouk, S. Katsouba, A. Demianovich, V. Stanovski, S. Voitech, V. Vysotski, and V. Ponomar, Solid-State Electron. **44**, 815 (2000).
[15]S. Lazarouk, S. Katsouba, A. Leshok, A. Demianovich, V. Stanovski, S. Voitech, V. Vysotski, and V. Ponomar, Microelectron. Eng. **50**, 321 (2000).
[16]S. K. Lazarouk, P. V. Jaguiro, A. A. Leshok, and V. E. Borisenko, Physica E (Amsterdam) **16**, 495 (2003).
[17]S. K. Lazarouk, A. A. Leshok, V. A. Labunov, and V. E. Borisenko, Fiz. Tekh. Poluprovodn. **39**, 149 (2005) [Semiconductors **39**, 136 (2005)].
[18]S. Lazarouk, P. Jaguiro, S. Katsouba, G. Masini, S. La Monica, G. Maiello, and A. Ferrari, Appl. Phys. Lett. **68**, 2108 (1996).
[19]S. K. Lazarouk, D. A. Sasinovich, P. S. Katsuba, V. A. Labunov, A. A. Leshok, and V. E. Borisenko, Fiz. Tekh. Poluprovodn. **41**, 1109 (2007) [Semicond. **41**, 1109 (2007)].

Downloaded 23 Apr 2010 to 143.89.47.22. Redistribution subject to AIP license or copyright; see http://jap.aip.org/jap/copyright.jsp